
Attend and Predict: Understanding Gene Regulation by Selective Attention on Chromatin

Ritambhara Singh, Jack Lanchantin, Arshdeep Sekhon, Yanjun Qi
Department of Computer Science
University of Virginia
yanjun@virginia.edu

Abstract

The past decade has seen a revolution in genomic technologies that enabled a flood of genome-wide profiling of chromatin marks. Recent literature tried to understand gene regulation by predicting gene expression from large-scale chromatin measurements. Two fundamental challenges exist for such learning tasks: (1) genome-wide chromatin signals are spatially structured, high-dimensional and highly modular; and (2) the core aim is to understand what the relevant factors are and how they work together. Previous studies either failed to model complex dependencies among input signals or relied on separate feature analysis to explain the decisions. This paper presents an attention-based deep learning approach, AttentiveChrome, that uses a unified architecture to model and to interpret dependencies among chromatin factors for controlling gene regulation. AttentiveChrome uses a hierarchy of multiple Long Short-Term Memory (LSTM) modules to encode the input signals and to model how various chromatin marks cooperate automatically. AttentiveChrome trains two levels of attention jointly with the target prediction, enabling it to attend differentially to relevant marks and to locate important positions per mark. We evaluate the model across 56 different cell types (tasks) in humans. Not only is the proposed architecture more accurate, but its attention scores provide a better interpretation than state-of-the-art feature visualization methods such as saliency maps.¹

1 Introduction

Gene regulation is the process of how the cell controls which genes are turned “on” (expressed) or “off” (not-expressed) in its genome. The human body contains hundreds of different cell types, from liver cells to blood cells to neurons. Although these cells include the same set of DNA information, their functions are different². The regulation of different genes controls the destiny and function of each cell. In addition to DNA sequence information, many factors, especially those in its environment (i.e., chromatin), can affect which genes the cell expresses. This paper proposes an attention-based deep learning architecture to learn from data how different chromatin factors influence gene expression in a cell. Such understanding of gene regulation can enable new insights into principles of life, the study of diseases, and drug development.

“Chromatin” denotes DNA and its organizing proteins³. A cell uses specialized proteins to organize DNA in a condensed structure. These proteins include histones, which form “bead“-like structures that DNA wraps around, in turn organizing and compressing the DNA. An important aspect of histone proteins is that they are prone to chemical modifications that can change the spatial arrangement of

¹Code shared at www.deepchrome.org.

²DNA is a long string of paired chemical molecules or nucleotides that fall into four different types and are denoted as A, T, C, and G. DNA carries information organized into units such as genes. The set of genetic material of DNA in a cell is called its genome.

³The complex of DNA, histones, and other structural proteins is called chromatin.

DNA. These spatial re-arrangements result in certain DNA regions becoming accessible or restricted and therefore affecting expressions of genes in the neighborhood region. Researchers have established the “Histone Code Hypothesis” that explores the role of histone modifications in controlling gene regulation. Unlike genetic mutations, chromatin changes such as histone modifications are potentially reversible ([5]). This crucial difference makes the understanding of how chromatin factors determine gene regulation even more impactful because this knowledge can help developing drugs targeting genetic diseases.

At the whole genome level, researchers are trying to chart the locations and intensities of all the chemical modifications, referred to as marks, over the chromatin ⁴. Recent advances in next-generation sequencing have allowed biologists to profile a significant amount of gene expression and chromatin patterns as signals (or read counts) across many cell types covering the full human genome. These datasets have been made available through large-scale repositories, the latest being the Roadmap Epigenome Project (REMC, publicly available) ([18]). REMC recently released 2,804 genome-wide datasets, among which 166 datasets are gene expression reads (RNA-Seq datasets) and the rest are signal reads of various chromatin marks across 100 different “normal” human cells/tissues [18].

The fundamental aim of processing and understanding this repository of “big” data is to understand gene regulation. For each cell type, we want to know which chromatin marks are the most important and how they work together in controlling gene expression. However, previous machine learning studies on this task either failed to model spatial dependencies among marks or required additional feature analysis to explain the predictions (Section 4). Computational tools should consider two important properties when modeling such data.

- First, signal reads for each mark are spatially structured and high-dimensional. For instance, to quantify the influence of a histone modification mark, learning methods typically need to use as input features all of the signals covering a DNA region of length 10,000 base pair (bp) ⁵ centered at the transcription start site (TSS) of each gene. These signals are sequentially ordered along the genome direction. To develop “epigenetic” drugs, it is important to recognize how a chromatin mark’s effect on regulation varies over different genomic locations.
- Second, various types of marks exist in human chromatin that can influence gene regulation. For example, each of the five standard histone proteins can be simultaneously modified at multiple different sites with various kinds of chemical modifications, resulting in a large number of different histone modification marks. For each mark, we build a feature vector representing its signals surrounding a gene’s TSS position. When modeling genome-wide signal reads from multiple marks, learning algorithms should take into account the modular nature of such feature inputs, where each mark functions as a module. We want to understand how the interactions among these modules influence the prediction (gene expression).

In this paper we propose an attention-based deep learning model, AttentiveChrome, that learns to predict the expression of a gene from an input of histone modification signals covering the gene’s neighboring DNA region. By using a hierarchy of multiple LSTM modules, AttentiveChrome can discover interactions among signals of each chromatin mark, and simultaneously learn complex dependencies among different marks. Two levels of “soft” attention mechanisms are trained, (1) to attend to the most relevant regions of a chromatin mark, and (2) to recognize and attend to the important marks. Through predicting and attending in one unified architecture, AttentiveChrome allows users to understand how chromatin marks control gene regulation in a cell. In summary, this work makes the following contributions:

- AttentiveChrome provides more accurate predictions than state-of-the-art baselines. Using datasets from REMC, we evaluate AttentiveChrome on 56 different cell types (tasks).
- We validate and compare interpretation scores using correlation to a new mark signal from REMC (not used in modeling). AttentiveChrome’s attention scores provide a better interpretation than state-of-the-art methods for visualizing deep learning models.
- AttentiveChrome can model highly modular inputs where each module is highly structured. AttentiveChrome can explain its decisions by providing “what” and “where” the model has focused

⁴In biology this field is called epigenetics. “Epi” in Greek means over. The epigenome in a cell is the set of chemical modifications over the chromatin that alter gene expression.

⁵A base pair refers to one of the double-stranded DNA sequence characters (ACGT)

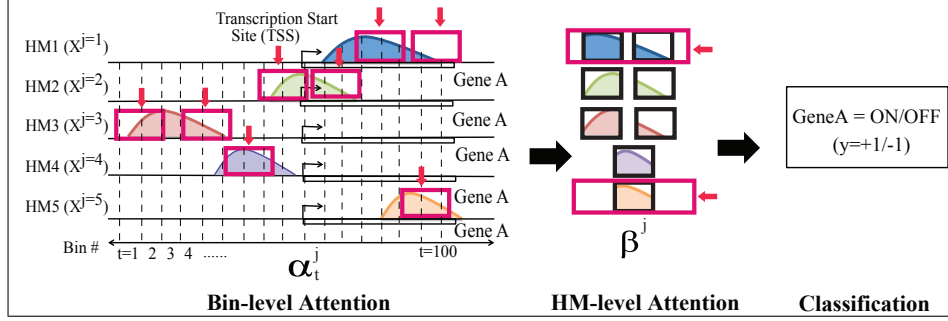


Figure 1: Overview of the proposed AttentiveChrome framework. It includes 5 important parts: (1) Bin-level LSTM encoder for each HM mark; (2) Bin-level α -Attention across all bin positions of each HM mark; (3) HM-level LSTM encoder encoding all HM marks; (4) HM-level β -Attention among all HM marks; (5) the final classification.

on. This flexibility and interpretability make this model an ideal approach for many real-world applications.

- To the authors’ best knowledge, AttentiveChrome is the first attention-based deep learning method for modeling data from molecular biology.

In the following sections, we denote vectors with bold font and matrices using capital letters. To simplify notation, we use “HM” as a short form for the term “histone modification”.

2 Background: Long Short-Term Memory (LSTM) Networks

Recurrent neural networks (RNNs) have been widely used in applications such as natural language processing due to their abilities to model sequential dependencies. Given an input matrix \mathbf{X} of size $n_{in} \times T$, an RNN produces a matrix \mathbf{H} of size $d \times T$, where n_{in} is the input feature size, T is the length of input feature, and d is the RNN embedding size. At each timestep $t \in \{1, \dots, T\}$, an RNN takes an input column vector $\mathbf{x}_t \in \mathbb{R}^{n_{in}}$ and the previous hidden state vector $\mathbf{h}_{t-1} \in \mathbb{R}^d$ and produces the next hidden state \mathbf{h}_t by applying the following recursive operation:

$$\mathbf{h}_t = \sigma(\mathbf{W}\mathbf{x}_t + \mathbf{U}\mathbf{h}_{t-1} + \mathbf{b}) = \overrightarrow{LSTM}(\mathbf{x}_t), \quad (1)$$

where \mathbf{W} , \mathbf{U} , \mathbf{b} are the trainable parameters of the model, and σ is an element-wise nonlinearity function. Due to the recursive nature, RNNs can capture the complete set of dependencies among all timesteps being modeled, like all spatial positions in a sequential sample. To handle the “vanishing gradient” issue of training basic RNNs, Hochreiter *et al.* [13] proposed an RNN variant called the Long Short-term Memory (LSTM) network.

An LSTM layer has an input-to-state component and a recurrent state-to-state component like that in Eq. (1). Additionally, it has gating functions that control when information is written to, read from, and forgotten. Though the LSTM formulation results in a complex form of Eq. (1) (see Supplementary), when given input vector \mathbf{x}_t and the state \mathbf{h}_{t-1} from previous time step $t - 1$, an LSTM module also produces a new state \mathbf{h}_t . The embedding vector \mathbf{h}_t encodes the learned representation summarizing feature dependencies from the time step 0 to the time step t . For our task, we call each bin position on the genome coordinate a “time step”.

3 AttentiveChrome: A Deep Model for Joint Classification and Visualization

Input and output formulation for the task: We use the same feature inputs and outputs as done previously in DeepChrome ([29]). Following Cheng *et al.* [7], the gene expression prediction is formulated as a binary classification task whose output represents if the gene expression of a gene is high(+1) or low(-1). As shown in Figure 1, the input feature of a sample (a particular gene) is denoted as a matrix \mathbf{X} of size $M \times T$. Here M denotes the number of HM marks we consider in the input. T is the total number of bin positions we take into account from the neighboring region of a gene’s TSS site on the genome. We refer to this region as the ‘gene region’ in the rest of the paper. \mathbf{x}^j denotes the j -th row vector of \mathbf{X} whose elements are sequentially structured (signals from the j -th HM mark) $j \in \{1, \dots, M\}$. x_t^j in matrix \mathbf{X} represents the signal from the t -th bin of the j -th HM

mark. $t \in \{1, \dots, T\}$. We assume our training set D contains N_{tr} labeled pairs. We denote the n -th pair as $(\mathbf{X}^{(n)}, y^{(n)})$, $\mathbf{X}^{(n)}$ is a matrix of size $M \times T$ and $y^{(n)} \in \{-1, +1\}$, where $n \in \{1, \dots, N_{tr}\}$.

An end-to-end deep architecture for predicting and attending jointly: AttentiveChrome learns to predict the expression of a gene from an input of HM signals covering its gene region. First, the signals of each HM mark are fed into a separate LSTM network to encode the spatial dependencies among its bin signals, and then another LSTM is used to model how multiple factors work together for predicting gene expression. Two levels of "soft" attention mechanisms are trained and dynamically predicted for each gene: (1) to attend to the most relevant positions of an HM mark, and (2) then to recognize and attend to the relevant marks. In summary, AttentiveChrome consists of five main modules (see Supplementary Figure S:2): (1) Bin-level LSTM encoder for each HM mark; (2) Bin-level Attention on each HM mark; (3) HM-level LSTM encoder encoding all HM marks; (4) HM-level Attention over all the HM marks; (5) the final classification module. We describe the details of each component as follows:

Bin-Level Encoder Using LSTMs: For a gene of interest, the j -th row vector, \mathbf{x}^j , from \mathbf{X} includes a total of T elements that are sequentially ordered along the genome coordinate. Considering the sequential nature of such signal reads, we treat each element (essentially a bin position) as a 'time step' and use a bidirectional LSTM to model the complete dependencies among elements in \mathbf{x}^j . A bidirectional LSTM contains two LSTMs, one in each direction (see Supplementary Figure S:2 (c)). It includes a forward \overrightarrow{LSTM}^j that models \mathbf{x}^j from x_1^j to x_T^j and a backward \overleftarrow{LSTM}^j that models from x_T^j to x_1^j . For each position t , the two LSTMs output $\overrightarrow{\mathbf{h}}_t^j$ and $\overleftarrow{\mathbf{h}}_t^j$, each of size d . $\overrightarrow{\mathbf{h}}_t^j = \overrightarrow{LSTM}^j(x_t^j)$ and $\overleftarrow{\mathbf{h}}_t^j = \overleftarrow{LSTM}^j(x_t^j)$. The final embedding vector at the t -th position is the concatenation $\mathbf{h}_t^j = [\overrightarrow{\mathbf{h}}_t^j, \overleftarrow{\mathbf{h}}_t^j]$.

By coupling these LSTM-based HM encoders with the final classification, they can learn to embed each HM mark by extracting the dependencies among bins that are essential for the prediction task.

Bin-Level Attention, α -attention: Although the LSTM can encode dependencies among the bins, it is difficult to determine which bins are *most important* for prediction from the LSTM. To automatically and adaptively highlight the most relevant bins for each sample, we use "soft" attention to learn the importance weights of bins. This means when representing j -th HM mark, AttentiveChrome follows a basic concept that not all bins contribute equally to the encoding of the entire j -th HM mark. The attention mechanism can help locate and recognize those bins that are important for the current gene sample of interest from j -th HM mark and can aggregate those important bins to form an embedding vector. This extraction is implemented through learning a weight vector α^j of size T for the j -th HM mark. For $t \in \{1, \dots, T\}$, α_t^j represents the importance of the t -th bin in the j -th HM. It is computed as: $\alpha_t^j = \frac{\exp(\mathbf{W}_b \mathbf{h}_t^j)}{\sum_{i=1}^T \exp(\mathbf{W}_b \mathbf{h}_i^j)}$.

α_t^j is a scalar and is computed by considering all bins' embedding vectors $\{\mathbf{h}_1^j, \dots, \mathbf{h}_T^j\}$. The context parameter \mathbf{W}_b is randomly initialized and jointly learned with the other model parameters during training. Our intuition is that through \mathbf{W}_b the model will automatically learn the context of the task (e.g., type of a cell) as well as the positional relevance to the context simultaneously. Once we have the importance weight of each bin position, we can represent the entire j -th HM mark as a weighted sum of all its bin embeddings: $\mathbf{m}^j = \sum_{t=1}^T \alpha_t^j \times \mathbf{h}_t^j$. Essentially the attention weights α_t^j tell us the relative importance of the t -th bin in the representation \mathbf{m}^j for the current input \mathbf{X} (both \mathbf{h}_t^j and α_t^j depend on \mathbf{X}).

HM-Level Encoder Using Another LSTM: We aim to capture the dependencies among HMs as some HMs are known to work together to repress or activate gene expression [6]. Therefore, next we model the joint dependencies among multiple HM marks (essentially, learn to represent a set). Even though there exists no clear order among HMs, we assume an imagined sequence as $\{HM_1, HM_2, HM_3, \dots, HM_M\}$ ⁶. We implement another bi-directional LSTM encoder, this time on the imagined sequence of HMs using the representations \mathbf{m}^j of the j -th HMs as LSTM inputs (Supplementary Figure S:2 (e)). Setting the embedding size as d' , this set-based encoder, we denote as $LSTM_s$, encodes the j -th HM as: $\mathbf{s}^j = [\overrightarrow{LSTM}_s(\mathbf{m}^j), \overleftarrow{LSTM}_s(\mathbf{m}^j)]$. Differently from \mathbf{m}^j , \mathbf{s}^j encodes the dependencies between the j -th HM and other HM marks.

⁶We tried several different architectures to model the dependencies among HMs, and found no clear ordering.

Table 1: Comparison of previous studies for the task of quantifying gene expression using histone modification marks (adapted from [29]). AttentiveChrome is the only model that exhibits all 8 desirable properties.

Computational Study	Unified	Non-linear	Bin-Info	Representation Learning		Prediction	Feature Inter.	Interpretable
				Neighbor Bins	Whole Region			
Linear Regression ([14])	×	×	×	×	✓	✓	×	✓
Support Vector Machine ([7])	×	✓	Bin-specific	×	✓	✓	✓	×
Random Forest ([10])	×	✓	Best-bin	×	✓	×	×	×
Rule Learning ([12])	×	✓	×	×	✓	×	✓	×
DeepChrome-CNN [29]	✓	✓	Automatic	✓	✓	✓	✓	×
AttentiveChrome	✓	✓	Automatic	✓	✓	✓	✓	✓

HM-Level Attention, β -attention: Now we want to focus on the important HM markers for classifying a gene’s expression as high or low. We do this by learning a second level of attention among HMs. Similar to learning α_t^j , we learn another set of weights β^j for $j \in \{1, \dots, M\}$ representing the importance of HM^j . β^i is calculated as: $\beta^j = \frac{\exp(\mathbf{W}_s \mathbf{s}^j)}{\sum_{i=1}^M \exp(\mathbf{W}_s \mathbf{s}^i)}$. The *HM-level* context parameter \mathbf{W}_s learns the context of the task and learns how HMs are relevant to that context. \mathbf{W}_s is randomly initialized and jointly trained. We encode the entire "gene region" into a hidden representation \mathbf{v} as a weighted sum of embeddings from all HM marks: $\mathbf{v} = \sum_{j=1}^M \beta^j \mathbf{s}^j$. We can interpret the learned attention weight β^i as the relative importance of HM^i when blending all HM marks to represent the entire gene region for the current gene sample \mathbf{X} .

Training AttentiveChrome End-to-End: The vector \mathbf{v} summarizes the information of all HMs for a gene sample. We feed it to a simple classification module f (Supplementary Figure S:2(f)) that computes the probability of the current gene being expressed high or low: $f(\mathbf{v}) = \text{softmax}(\mathbf{W}_c \mathbf{v} + b_c)$. \mathbf{W}_c and b_c are learnable parameters. Since the entire model, including the attention mechanisms, is differentiable, learning end-to-end is trivial by using backpropagation [21]. All parameters are learned together to minimize a negative log-likelihood loss function that captures the difference between true labels y and predicted scores from $f(\cdot)$.

4 Connecting to Previous Studies

In recent years, there has been an explosion of deep learning models that have led to groundbreaking performance in many fields such as computer vision [17], natural language processing [30], and computational biology [1, 27, 38, 16, 19, 29].

Attention-based deep models: The idea of attention in deep learning arises from the properties of the human visual system. When perceiving a scene, the human vision gives more importance to some areas over others [9]. This adaptation of "attention" allows deep learning models to focus selectively on only the important features. Deep neural networks augmented with attention mechanisms have obtained great success on multiple research topics such as machine translation [4], object recognition [2, 26], image caption generation [33], question answering [30], text document classification [34], video description generation [35], visual question answering [32], or solving discrete optimization [31]. Attention brings in two benefits: (1) By selectively focusing on parts of the input during prediction the attention mechanisms can reduce the amount of computation and the number of parameters associated with deep learning model [2, 26]. (2) Attention-based modeling allows for learning salient features dynamically as needed [34], which can help improve accuracy.

Different attention mechanisms have been proposed in the literature, including ‘soft’ attention [4], ‘hard’ attention [33, 24], or ‘location-aware’ [8]. Soft attention [4] calculates a ‘soft’ weighting scheme over all the component feature vectors of input. These weights are then used to compute a weighted combination of the candidate feature vectors. The magnitude of an attention weight correlates highly with the degree of significance of the corresponding component feature vector to the prediction. Inspired by [34], AttentiveChrome uses two levels of soft attention for predicting gene expression from HM marks.

Visualizing and understanding deep models: Although deep learning models have proven to be very accurate, they have widely been viewed as “black boxes”. Researchers have attempted to develop separate visualization techniques that explain a deep classifier’s decisions. Most prior studies have focused on understanding convolutional neural networks (CNN) for image classifications, including techniques such as “deconvolution” [36], “saliency maps” [3, 28] and “class optimization” based

visualisation [28]. The “deconvolution” approach [36] maps hidden layer representations back to the input space for a specific example, showing those features of an image that are important for classification. “Saliency maps” [28] use a first-order Taylor expansion to linearly approximate the deep network and seek most relevant input features. The “class optimization” based visualization [28] tries to find the best example (through optimization) that maximizes the probability of the class of interest. Recent studies [15, 22] explored the interpretability of recurrent neural networks (RNN) for text-based tasks. Moreover, since attention in models allows for automatically extracting salient features, attention-coupled neural networks impart a degree of interpretability. By visualizing what the model attends to in [34], attention can help gauge the predictive importance of a feature and hence interpret the output of a deep neural network.

Deep learning in bioinformatics: Deep learning is steadily gaining popularity in the bioinformatics community. This trend is credited to its ability to extract meaningful representations from large datasets. For instance, multiple recent studies have successfully used deep learning for modeling protein sequences [23, 37] and DNA sequences [1, 20], predicting gene expressions [29], as well as understanding the effects of non-coding variants [38, 27].

Previous machine learning models for predicting gene expression from histone modification marks: Multiple machine learning methods have been proposed to predict gene expression from histone modification data (surveyed by Dong *et al.* [11]) including linear regression [14], support vector machines [7], random forests [10], rule-based learning [12] and CNNs [29]. These studies designed different feature selection strategies to accommodate a large amount of histone modification signals as input. The strategies vary from using signal averaging across all relevant positions, to a ‘best position’ strategy that selected the input signals at the position with the highest correlation to the target gene expression and automatically learning combinatorial interactions among histone modification marks using CNN (called DeepChrome [29]). DeepChrome outperformed all previous methods (see Supplementary) on this task and used a class optimization-based technique for visualizing the learned model. However, this class-level visualization lacks the necessary granularity to understand the signals from multiple chromatin marks at the individual gene level.

Table 1 compares previous learning studies on the same task with AttentiveChrome across seven desirable model properties. The columns indicate properties (1) whether the study has a unified end-to-end architecture or not, (2) if it captures non-linearity among features, (3) how has the bin information been incorporated, (4) if representation of features is modeled on local and (5) global scales, (6) whether gene expression prediction is provided, (7) if combinatorial interactions among histone modifications are modeled, and finally (8) if the model is interpretable. AttentiveChrome is the only model that exhibits all seven properties. Additionally, Section 5 compares the attention weights from AttentiveChrome with the visualization from “saliency map” and “class optimization.” Using the correlation to one additional HM mark from REMC, we show that AttentiveChrome provides better interpretation and validation.

5 Experiments and Results

Dataset: Following DeepChrome [29], we downloaded gene expression levels and signal data of five core HM marks for 56 different cell types archived by the REMC database [18]. Each dataset contains information about both the location and the signal intensity for a mark measured across the whole genome. The selected five core HM marks have been uniformly profiled across all 56 cell types in the REMC study [18]. These five HM marks include (we rename these HMs in our analysis for readability): H3K27me3 as H_{reprA} , H3K36me3 as H_{struct} , H3K4me1 as H_{enhc} , H3K4me3 as H_{prom} , and H3K9me3 as H_{reprB} . HMs H_{reprA} and H_{reprB} are known to repress the gene expression, H_{prom} activates gene expression, H_{struct} is found over the gene body, and H_{enhc} sometimes helps in activating gene expression.

Details of the Dataset: We divided the 10,000 base pair DNA region (± 5000 bp) around the transcription start site (TSS) of each gene into bins, with each bin containing 100 continuous bp). For each gene in a specific celltype, the feature generation process generated a 5×100 matrix, \mathbf{X} , where columns represent $T (= 100)$ different bins and rows represent $M (= 5)$ HMs. For each cell type, the gene expression has been quantified for all annotated genes in the human genome and has been normalized. As previously mentioned, we formulated the task of gene expression prediction as a binary classification task. Following [7], we used the median gene expression across all genes for a particular cell type as the threshold to discretize expression values. For each cell type, we divided

Table 2: AUC score performances for different variations of AttentiveChrome and baselines

	Baselines		AttentiveChrome Variations				
Model	DeepChrome (CNN) [29]	LSTM	CNN-Attn	CNN- α, β	LSTM-Attn	LSTM- α	LSTM- α, β
Mean	0.8008	0.8052	0.7622	0.7936	0.8100	0.8133	0.8115
Median	0.8009	0.8036	0.7617	0.7914	0.8118	0.8143	0.8123
Max	0.9225	0.9185	0.8707	0.9059	0.9155	0.9218	0.9177
Min	0.6854	0.7073	0.6469	0.7001	0.7237	0.7250	0.7215
Improvement over DeepChrome [29] (out of 56 cell types)		36	0	16	49	50	49

our set of 19,802 gene samples into three separate, but equal-size folds for training (6601 genes), validation (6601 genes), and testing (6600 genes) respectively.

Model Variations and Two Baselines: In Section 3, we introduced three main components of AttentiveChrome to handle the task of predicting gene expression from HM marks: LSTMs, attention mechanisms, and hierarchical attention. To investigate the performance of these components, our experiments compare multiple AttentiveChrome model variations plus two standard baselines.

- DeepChrome [29]: The temporal (1-D) CNN model used by Singh *et al.* [29] for the same classification task. This study did not consider the modular property of HM marks.
- LSTM: We directly apply an LSTM on the input matrix \mathbf{X} without adding any attention. This setup does not consider the modular property of each HM mark, that is, we treat the signals of all HMs at t -th bin position as the t -th input to LSTM.
- LSTM-Attn: We add one attention layer on the baseline LSTM model over input \mathbf{X} . This setup does not consider the modular property of HM marks.
- CNN-Attn: We apply one attention layer over the CNN model from DeepChrome [29], after removing the max-pooling layer to allow bin-level attention for each bin. This setup does not consider the modular property of HM marks.
- LSTM- α, β : As introduced in Section 3, this model uses one LSTM per HM mark and add one α -attention per mark. Then it uses another level of LSTM and β -attention to combine HMs.
- CNN- α, β : This considers the modular property among HM marks. We apply one CNN per HM mark and add one α -attention per mark. Then it uses another level of CNN and β -attention to combine HMs.
- LSTM- α : This considers the modular property of HM marks. We apply one LSTM per HM mark and add one α -attention per mark. Then, the embedding of HM marks is concatenated as one long vector and then fed to a 2-layer fully connected MLP.

We use datasets across 56 cell types, comparing the above methods over each of the 56 different tasks.

Model Hyperparameters: For AttentiveChrome variations, we set the bin-level LSTM embedding size d to 32 and the HM-level LSTM embedding size as 16. Since we implement a bi-directional LSTM, this results in each embedding vector \mathbf{h}_t as size 64 and embedding vector \mathbf{m}_j as size 32. Therefore, we set the context vectors, \mathbf{W}_b and \mathbf{W}_s , to size 64 and 32 respectively.⁷

Performance Evaluation: Table 2 compares different variations of AttentiveChrome using summarized AUC scores across all 56 cell types on the test set. We find that overall the LSTM-attention based models perform better than CNN-based and LSTM baselines. CNN-attention model gives worst performance. To add the bin-level attention layer to the CNN model, we removed the max-pooling layer. We hypothesize that the absence of max-pooling is the cause behind its low performance. LSTM- α has better empirical performance than the LSTM- α, β model. We recommend the use of the proposed AttentiveChrome LSTM- α, β (from here on referred to as AttentiveChrome) for hypothesis generation because it provides a good trade-off between AUC and interpretability. Also, while the performance improvement over DeepChrome [29] is not large, AttentiveChrome is better as it allows interpretability to the "black box" neural networks.

⁷We can view \mathbf{W}_b as 1×64 matrix.

Table 3: Pearson Correlation values between weights assigned for H_{prom} (active HM) by different visualization techniques and H_{active} read coverage (indicating actual activity near "ON" genes) for predicted "ON" genes across three major cell types.

Viz. Methods	H1-hESC	GM12878	K562
α Map (LSTM- α)	0.8523	0.8827	0.9147
α Map (LSTM- α, β)	0.8995	0.8456	0.9027
Class-based Optimization (CNN)	0.0562	0.1741	0.1116
Saliency Map (CNN)	0.1822	-0.1421	0.2238

Using Attention Scores for Interpretation: Unlike images and text, the results for biology are hard to interpret by just looking at them. Therefore, we use additional evidence from REMC as well as introducing a new strategy to qualitatively and quantitatively evaluate the bin-level attention weights or α -map LSTM- α model and AttentiveChrome. To specifically validate that the model is focusing its attention at the right bins, we use the read counts of a new HM signal - H3K27ac from REMC database. We represent this HM as H_{active} because this HM marks the region that is active when the gene is "ON". H3K27ac is an important indication of activity in the DNA regions and is a good source to validate the results. We did not include H3K27ac Mark as input because it has not been profiled for all 56 cell types we used for prediction. However, the genome-wide reads of this HM mark are available for three important cell types in the blood lineage: H1-hESC (stem cell), GM12878 (blood cell), and K562 (leukemia cell). We, therefore, chose to compare and validate interpretation in these three cell types. This HM signal has not been used at any stage of the model training or testing. We use it solely to analyze the visualization results.

We use the average read counts of H_{active} across all 100 bins and for all the active genes (gene=ON) in the three selected cell types to compare different visualization methods. We compare the attention α -maps of the best performing LSTM- α and AttentiveChrome models with the other two popular visualization techniques: (1) the Class-based optimization method and (2) the Saliency map applied on the baseline DeepChrome-CNN model. We take the importance weights calculated by all visualization methods for our active input mark, H_{prom} , across 100 bins and then calculate their Pearson correlation to H_{active} counts across the same 100 bins. H_{active} counts indicate the actual active regions. Table 3 reports the correlation coefficients between H_{prom} weights and read coverage of H_{active} . We observe that attention weights from our models consistently achieve the highest correlation with the actual active regions near the gene, indicating that this method can capture the important signals for predicting gene activity. Interestingly, we observe that the saliency map on the DeepChrome achieves a higher correlation with H_{active} than the Class-based optimization method for two cell types: H1-hESC (stem cell) and K562 (leukemia cell).

Next, we obtain the attention weights learned by AttentionChrome, representing the important bins and HMs for each prediction of a particular gene as ON or OFF. For a specific gene sample, we can visualize and inspect the bin-level and HM-level attention vectors α_t^j and β^j generated by AttentionChrome. In Figure 2(a), we plot the average bin-level attention weights for each HM for cell type GM12878 (blood cell) by averaging α -maps of all predicted "ON" genes (top) and "OFF" genes (bottom). We see that on average for "ON" genes, the attention profiles near the TSS region are well defined for H_{prom} , H_{enhc} , and H_{struct} . On the contrary, the weights are low and close to uniform for H_{reprA} and H_{reprB} . This average trend reverses for "OFF" genes in which H_{reprA} and H_{reprB} seem to gain more importance over H_{prom} , H_{enhc} , and H_{struct} . These observations make sense biologically as H_{prom} , H_{enhc} , and H_{struct} are known to encourage gene activation while H_{reprA} and H_{reprB} are known to repress the genes⁸. On average, while H_{prom} is concentrated near the TSS region, other HMs like H_{struct} show a broader distribution away from the TSS. In summary, the importance of each HM and its position varies across different genes. E.g., H_{enhc} can affect a gene from a distant position.

In Figure 2(b), we plot the average read coverage of H_{active} (top) for the same 100 bins, that we used for input signals, across all the active genes (gene=ON) for GM12878 cell type. We also plot the bin-level attention weights α_t^j for AttentiveChrome (bottom) averaged over all genes predicted as ON for GM12878. Visually, we can tell that the average H_{prom} profile is similar to H_{active} . This

⁸The small dips at the TSS in both subfigures of Figure 2(a) are caused by missing signals at the TSS due to the inherent nature of the sequencing experiments.

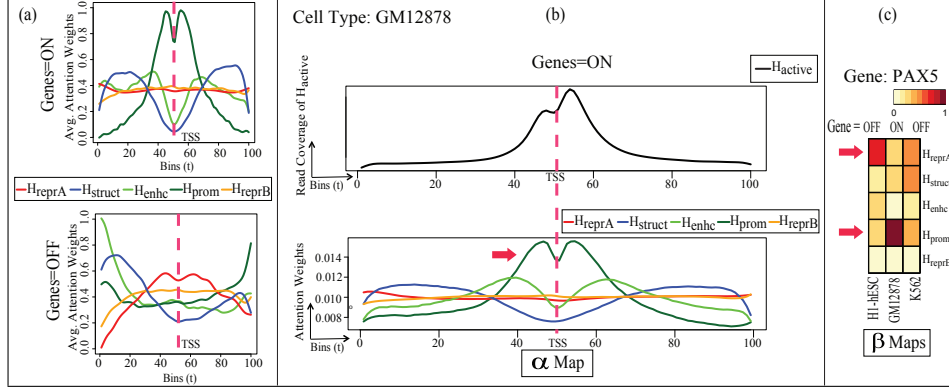


Figure 2: (Best viewed in color) (a) Bin-level attention weights (α_t^j) from AttentiveChrome averaged for all genes when predicting gene=ON and gene=OFF in GM12878 cell type. (b) Top: Cumulative H_{active} signal across all active genes. Bottom: Plot of the bin-level attention weights (α_t^j). These weights are averaged for gene=ON predictions. H_{prom} weights are concentrated near the TSS and corresponds well with the H_{active} indicating actual activity near the gene. This indicates that AttentiveChrome is focusing on the correct bin positions for this case (c) Heatmaps visualizing the HM-level weights (β^j), with $j \in \{1, \dots, 5\}$ for an important differentially regulated gene (PAX5) across three blood lineage cell types: H1-hESC (stem cell), GM12878 (blood cell), and K562 (leukemia cell). The trend of HM-level β^j weights for PAX5 have been verified through biological literature.

observation makes sense because H_{prom} is related to active regions for “ON” genes. Thus, validating our results from Table 3.

Finally in Figure 2(c) we demonstrate the advantage of AttentiveChrome over LSTM- α model by printing out the β^j weights for genes with differential expressions across the three cell types. That is, we select genes with varying ON(+1)/OFF(-1) states across the three chosen cell types using a heatmap. Figure 2(c) visualizes the β^j weights for a certain differentially regulated gene, PAX5. PAX5 is critical for the gene regulation when stem cells convert to blood cells ([25]). This gene is OFF in the H1-hESC cell stage (left column) but turns ON when the cell develops into GM12878 cell (middle column). The β^j weight of repressor mark H_{reprA} is high when gene=OFF in H1-hESC (left column). This same weight decreases when gene=ON in GM12878 (middle column). In contrast, the β^j weight of the promoter mark H_{prom} increases from H1-hESC (left column) to GM12878 (middle column). These trends have been observed in [25] showing that PAX5 relates to the conversion of chromatin states: from a repressive state ($H_{prom}(H3K4me3):-$, $H_{reprA}(H3K27me3):+$) to an active state ($H_{prom}(H3K4me3):+$, $H_{reprA}(H3K27me3):-$). This example shows that our β^j weights visualize how different HMs work together to influence a gene’s state (ON/OFF). We would like to emphasize that the attention weights on both bin-level (α -map) and HM-level (β -map) are gene (i.e. sample) specific.

The proposed AttentiveChrome model provides an opportunity for a plethora of downstream analyses that can help us understand the epigenomic mechanisms better. Besides, relevant datasets are big and noisy. A predictive model that automatically selects and visualizes essential features can significantly reduce the potential manual costs.

6 Conclusion

We have presented AttentiveChrome, an attention-based deep-learning approach that handles prediction and understanding in one architecture. The advantages of this work include:

- AttentiveChrome provides more accurate predictions than state-of-the-art baselines (Table 2).
- The attention scores of AttentiveChrome provide a better interpretation than saliency map and class optimization (Table 3). This allows us to view what the model ‘sees’ when making its prediction.
- AttentiveChrome can model highly modular feature inputs in which each is sequentially structured.
- To the authors’ best knowledge, AttentiveChrome is the first implementation of deep attention mechanism for understanding data about gene regulation. We can gain insights and understand the predictions by locating ‘what’ and ‘where’ AttentiveChrome has focused (Figure 2). Many real-world applications are seeking such knowledge from data.

References

- [1] Babak Alipanahi, Andrew DeLong, Matthew T Weirauch, and Brendan J Frey. Predicting the sequence specificities of dna-and rna-binding proteins by deep learning. Nature Publishing Group, 2015.
- [2] Jimmy Ba, Volodymyr Mnih, and Koray Kavukcuoglu. Multiple object recognition with visual attention.
- [3] David Baehrens, Timon Schroeter, Stefan Harmeling, Motoaki Kawanabe, Katja Hansen, and Klaus-Robert MÅzller. How to explain individual classification decisions. volume 11, pages 1803–1831, 2010.
- [4] Dzmitry Bahdanau, Kyunghyun Cho, and Yoshua Bengio. Neural machine translation by jointly learning to align and translate. *arXiv preprint arXiv:1409.0473*, 2014.
- [5] Andrew J Bannister and Tony Kouzarides. Regulation of chromatin by histone modifications. *Cell research*, 21(3):381–395, 2011.
- [6] Joanna Boros, Nausica Arnoult, Vincent Stroobant, Jean-François Collet, and Anabelle Decottignies. Polycomb repressive complex 2 and h3k27me3 cooperate with h3k9 methylation to maintain heterochromatin protein 1 α at chromatin. *Molecular and cellular biology*, 34(19):3662–3674, 2014.
- [7] Chao Cheng, Koon-Kiu Yan, Kevin Y Yip, Joel Rozowsky, Roger Alexander, Chong Shou, Mark Gerstein, et al. A statistical framework for modeling gene expression using chromatin features and application to modencode datasets. *Genome Biol*, 12(2):R15, 2011.
- [8] Jan K Chorowski, Dzmitry Bahdanau, Dmitriy Serdyuk, Kyunghyun Cho, and Yoshua Bengio. Attention-based models for speech recognition. In C. Cortes, N. D. Lawrence, D. D. Lee, M. Sugiyama, and R. Garnett, editors, *Advances in Neural Information Processing Systems 28*, pages 577–585. Curran Associates, Inc., 2015.
- [9] Maurizio Corbetta and Gordon L Shulman. Control of goal-directed and stimulus-driven attention in the brain. *Nature reviews neuroscience*, 3(3):201–215, 2002.
- [10] Xianjun Dong, Melissa C Greven, Anshul Kundaje, Sarah Djebali, James B Brown, Chao Cheng, Thomas R Gingeras, Mark Gerstein, Roderic Guigó, Ewan Birney, et al. Modeling gene expression using chromatin features in various cellular contexts. *Genome Biol*, 13(9):R53, 2012.
- [11] Xianjun Dong and Zhiping Weng. The correlation between histone modifications and gene expression. *Epigenomics*, 5(2):113–116, 2013.
- [12] Bich Hai Ho, Rania Mohammed Kotb Hassen, and Ngoc Tu Le. Combinatorial roles of dna methylation and histone modifications on gene expression. In *Some Current Advanced Researches on Information and Computer Science in Vietnam*, pages 123–135. Springer, 2015.
- [13] Sepp Hochreiter and Jürgen Schmidhuber. Long short-term memory. volume 9, pages 1735–1780. MIT Press, 1997.
- [14] Rosa Karlić, Ho-Ryun Chung, Julia Lasserre, Kristian Vlahoviček, and Martin Vingron. Histone modification levels are predictive for gene expression. *Proceedings of the National Academy of Sciences*, 107(7):2926–2931, 2010.
- [15] Andrej Karpathy, Justin Johnson, and Fei-Fei Li. Visualizing and understanding recurrent networks. 2015.
- [16] David R Kelley, Jasper Snoek, and John L Rinn. Basset: Learning the regulatory code of the accessible genome with deep convolutional neural networks. Cold Spring Harbor Lab, 2016.
- [17] Alex Krizhevsky, Ilya Sutskever, and Geoffrey E Hinton. Imagenet classification with deep convolutional neural networks. In *Advances in neural information processing systems*, pages 1097–1105, 2012.
- [18] Anshul Kundaje, Wouter Meuleman, Jason Ernst, Misha Bilenky, Angela Yen, Alireza Heravi-Moussavi, Pouya Kheradpour, Zhizhuo Zhang, Jianrong Wang, Michael J Ziller, et al. Integrative analysis of 111 reference human epigenomes. *Nature*, 518(7539):317–330, 2015.
- [19] Jack Lanchantin, Ritambhara Singh, Zeming Lin, and Yanjun Qi. Deep motif: Visualizing genomic sequence classifications. 2016.
- [20] Jack Lanchantin, Ritambhara Singh, Beilun Wang, and Yanjun Qi. Deep motif dashboard: Visualizing and understanding genomic sequences using deep neural networks. *arXiv preprint arXiv:1608.03644*, 2016.
- [21] Yann LeCun, Léon Bottou, Yoshua Bengio, and Patrick Haffner. Gradient-based learning applied to document recognition. volume 86, pages 2278–2324. IEEE, 1998.

- [22] Jiwei Li, Xinlei Chen, Eduard Hovy, and Dan Jurafsky. Visualizing and understanding neural models in nlp. 2015.
- [23] Zeming Lin, Jack Lanchantin, and Yanjun Qi. Must-cnn: A multilayer shift-and-stitch deep convolutional architecture for sequence-based protein structure prediction. In *Thirtieth AAAI Conference on Artificial Intelligence*, 2016.
- [24] Minh-Thang Luong, Hieu Pham, and Christopher D. Manning. Effective approaches to attention-based neural machine translation. In *Empirical Methods in Natural Language Processing (EMNLP)*, pages 1412–1421, Lisbon, Portugal, September 2015. Association for Computational Linguistics.
- [25] Shane McManus, Anja Ebert, Giorgia Salvagiotto, Jasna Medvedovic, Qiong Sun, Ido Tamir, Markus Jaritz, Hiromi Tagoh, and Meinrad Busslinger. The transcription factor pax5 regulates its target genes by recruiting chromatin-modifying proteins in committed b cells. *The EMBO journal*, 30(12):2388–2404, 2011.
- [26] Volodymyr Mnih, Nicolas Heess, Alex Graves, and others. Recurrent models of visual attention. In *Advances in neural information processing systems*, pages 2204–2212.
- [27] Daniel Quang and Xiaohui Xie. Danq: a hybrid convolutional and recurrent deep neural network for quantifying the function of dna sequences. *Nucleic acids research*, 44(11):e107–e107, 2016.
- [28] Karen Simonyan, Andrea Vedaldi, and Andrew Zisserman. Deep inside convolutional networks: Visualising image classification models and saliency maps. 2013.
- [29] Ritambhara Singh, Jack Lanchantin, Gabriel Robins, and Yanjun Qi. Deepchrome: deep-learning for predicting gene expression from histone modifications. *Bioinformatics*, 32(17):i639–i648, 2016.
- [30] Ilya Sutskever, Oriol Vinyals, and Quoc V Le. Sequence to sequence learning with neural networks. In *Advances in neural information processing systems*, pages 3104–3112, 2014.
- [31] Oriol Vinyals, Meire Fortunato, and Navdeep Jaitly. Pointer networks. In C. Cortes, N. D. Lawrence, D. D. Lee, M. Sugiyama, and R. Garnett, editors, *Advances in Neural Information Processing Systems 28*, pages 2692–2700. Curran Associates, Inc., 2015.
- [32] Huijuan Xu and Kate Saenko. Ask, attend and answer: Exploring question-guided spatial attention for visual question answering. In *ECCV*, 2016.
- [33] Kelvin Xu, Jimmy Ba, Ryan Kiros, Kyunghyun Cho, Aaron C Courville, Ruslan Salakhutdinov, Richard S Zemel, and Yoshua Bengio. Show, attend and tell: Neural image caption generation with visual attention. In *ICML*, volume 14, pages 77–81, 2015.
- [34] Zichao Yang, Diyi Yang, Chris Dyer, Xiaodong He, Alex Smola, and Eduard Hovy. Hierarchical attention networks for document classification. 2016.
- [35] Li Yao, Atousa Torabi, Kyunghyun Cho, Nicolas Ballas, Christopher Pal, Hugo Larochelle, and Aaron Courville. Describing videos by exploiting temporal structure. In *Computer Vision (ICCV), 2015 IEEE International Conference on. IEEE*, 2015.
- [36] Matthew D Zeiler and Rob Fergus. Visualizing and understanding convolutional networks. In *Computer Vision–ECCV 2014*, pages 818–833. Springer, 2014.
- [37] Jian Zhou and Olga G Troyanskaya. Deep supervised and convolutional generative stochastic network for protein secondary structure prediction. *arXiv preprint arXiv:1403.1347*, 2014.
- [38] Jian Zhou and Olga G Troyanskaya. Predicting effects of noncoding variants with deep learning-based sequence model. volume 12, pages 931–934. Nature Publishing Group, 2015.

Attend and Predict: Understanding Gene Regulation by Selective Attention on Chromatin

Ritambhara Singh, Jack Lanchantin, Arshdeep Sekhon, Yanjun Qi
Department of Computer Science
University of Virginia
yanjun@virginia.edu

S:1 Supplementary Information

S:1.1 More about results

Importance of All HMs as input signals: Not all HMs carry the same information, and it is important to include different HMs for gene expression prediction. While H_{prom} may be essential to predict gene=ON, H_{enhc} may play a role to make that prediction. Contrarily, for "OFF" genes, HMs like H_{reprA} may play a significant role. To demonstrate this, we used only one HM at a time and performed the classification. The accuracy decreases when just one HM is used. Table S:1 shows AUC scores in GM12878 when all HMs are used as input signals and when we use them one at a time. We observe that the performance drops drastically, indicating that it is vital to include different HMs for gene expression prediction.

Table S:1: AUC scores in GM12878 when all HMs are used as input signals and when we use them one at a time. The AUC score reduces drastically, indicating that it is vital to include different HMs for gene expression prediction

HMs used as input	AUC Score
All 5 HMs	0.9085
H_{prom}	0.8893
H_{enhc}	0.8516
H_{struct}	0.8506
H_{reprA}	0.7698
H_{reprB}	0.6465

S:1.2 More about experimental settings

Evaluation Metric for Classification: We use the area under the receiver operating characteristic curve (AUC) as our evaluation metric. AUC represents the probability that a randomly selected 'event' will be regarded with greater suspicion than a randomly selected 'non-event'. AUC scores range between 0 and 1, with values closer to 1 indicating successful predictions.

Choice for Evaluation Metric: We also calculated the F1-scores for baseline DeepChrome[2] and AttentiveChrome, presented in Table S:2.

We observe that the F1-scores vary significantly across cell types. This is because, for most cell types, the number of samples with Gene=OFF are much more substantial (80% of Test data) than those with Gene=ON. Since AUC score, used in all previous works, is independent of the distribution of positive and negative classes and depends only on the learning model, we use it as our evaluation metric to measure performances of different models.

Table S:2: Performance comparison in terms of F1-scores

	DeepChrome[2]	AttChrome
Mean	0.55	0.56
Median	0.69	0.62
Max	0.89	0.88
Min	0.12	0.16

Choice of Baselines: We chose the DeepChrome CNN based model [2] as our baseline, as it has been shown to outperform SVM and Random Forest based models used previously for this task (reported in [2]) . We summarize performance results of all the baselines in Table S:3.

Table S:3: Performance comparison (in AUC Scores) of all baseline models

	RF	SVM	DeepChrome[2]	LSTM
Mean	0.59	0.75	0.80	0.81
Median	0.58	0.76	0.80	0.80
Max	0.71	0.87	0.92	0.92
Min	0.52	0.62	0.69	0.71

S:1.3 More about Method

Long Short-Term Memory (LSTM) Networks: Recurrent neural networks (RNNs) have been designed for modeling sequential data samples and are used widely in sequential data application tasks such as natural language processing. RNNs are advantageous over CNNs because they can capture the complete set of dependencies among spatial positions in a sequential sample.

Given an input matrix \mathbf{X} of size $n_{in} \times T$, an RNN produces a matrix \mathbf{H} of size $d \times T$, where n_{in} is the input feature size, T is the input feature length, and d is the RNN embedding size. At each timestep $t \in [1..T]$, an RNN takes an input column vector $\mathbf{x}_t \in \mathbb{R}^{n_{in}}$ and the previous hidden state vector $\mathbf{h}_{t-1} \in \mathbb{R}^d$ and produces the next hidden state \mathbf{h}_t by applying the following recursive operation:

$$\mathbf{h}_t = \sigma(\mathbf{W}\mathbf{x}_t + \mathbf{U}\mathbf{h}_{t-1} + \mathbf{b}), \quad (\text{S:1-1})$$

where \mathbf{W} , \mathbf{U} , \mathbf{b} are the trainable parameters of the model, and σ is an element-wise nonlinearity function. Due to their recursive nature, RNNs can model the full conditional distribution of any sequential data and find dependencies over time. To handle “vanishing gradient” issue of training basic RNNs, [1] proposed an RNN variant called the Long Short-term Memory (LSTM) network, which can handle long term dependencies by using gating functions. These gates can control when information

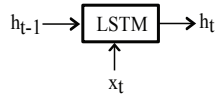


Figure S:1: A simple representation of an LSTM module.

is written to, read from, and forgotten. Specifically, LSTM “cells” take inputs \mathbf{x}_t , \mathbf{h}_{t-1} , and \mathbf{c}_{t-1} , and produce \mathbf{h}_t , and \mathbf{c}_t :

$$\begin{aligned} \mathbf{i}_t &= \sigma(\mathbf{W}^i \mathbf{x}_t + \mathbf{U}^i \mathbf{h}_{t-1} + \mathbf{b}^i) \\ \mathbf{f}_t &= \sigma(\mathbf{W}^f \mathbf{x}_t + \mathbf{U}^f \mathbf{h}_{t-1} + \mathbf{b}^f) \\ \mathbf{o}_t &= \sigma(\mathbf{W}^o \mathbf{x}_t + \mathbf{U}^o \mathbf{h}_{t-1} + \mathbf{b}^o) \\ \mathbf{g}_t &= \tanh(\mathbf{W}^g \mathbf{x}_t + \mathbf{U}^g \mathbf{h}_{t-1} + \mathbf{b}^g) \\ \mathbf{c}_t &= \mathbf{f}_t \odot \mathbf{c}_{t-1} + \mathbf{i}_t \odot \mathbf{g}_t \\ \mathbf{h}_t &= \mathbf{o}_t \odot \tanh(\mathbf{c}_t) \end{aligned}$$

where $\sigma(\cdot)$, $\tanh(\cdot)$, and \odot are element-wise sigmoid, hyperbolic tangent, and multiplication functions, respectively. \mathbf{i}_t , \mathbf{f}_t , and \mathbf{o}_t are the input, forget, and output gates, respectively.

Algorithm S:1 AttentiveChrome: Forward Propagation

Require: X ▷ Size: $M \times T$

- 1: **procedure** CLASSIFICATION(X)
- 2: $\{x_1^t, x_2^t, \dots, x_j^t\} \leftarrow X$ ▷ Size: $1 \times T$, $t \in \{1, \dots, T\}$ and $j \in \{1, \dots, M\}$
- 3: $\mathbf{m}^j \leftarrow \text{BinLevelAttention}(x_t^j)$
- 4: $\mathbf{v} \leftarrow \text{HMLLevelAttention}(\mathbf{m}^j)$
- 5: $y \leftarrow \text{MultiLayerPerceptron}(\mathbf{v})$
- 6: **return** y
- 7: **procedure** BIN-LEVEL ATTENTION(x_t^j)
- 8: **for** $j \in \{1, \dots, M\}$ **do** ▷ Run in Parallel
- 9: $\mathbf{h}_t^j \leftarrow \overrightarrow{LSTM}^j(x_t^j)$ ▷ Bi-directional LSTM
- 10: $\mathbf{h}_t^j \leftarrow \overleftarrow{LSTM}^j(x_t^j)$
- 11: $\mathbf{h}_t^j \leftarrow [\mathbf{h}_t^j, \mathbf{h}_t^j]$
- 12: $\alpha_t^j \leftarrow \frac{\exp(\mathbf{W}_b \mathbf{h}_t^j)}{\sum_{i=1}^T \exp(\mathbf{W}_b \mathbf{h}_i^j)}$ ▷ Size: $1 \times T$ for each $j \in \{1, \dots, M\}$
- 13: $\mathbf{m}^j \leftarrow \sum_{t=1}^T \alpha_t^j \times \mathbf{h}_t^j$
- 14: **return** \mathbf{m}^j
- 15: **procedure** HM-LEVEL ATTENTION(\mathbf{m}^j)
- 16: $\mathbf{s}^j \leftarrow [\overrightarrow{LSTM}_s(\mathbf{m}^j), \overleftarrow{LSTM}_s(\mathbf{m}^j)]$
- 17: $\beta^j \leftarrow \frac{\exp(\mathbf{W}_s \mathbf{s}^j)}{\sum_{i=1}^M \exp(\mathbf{W}_s \mathbf{s}^i)}$ ▷ Size: $1 \times M$
- 18: $\mathbf{v} \leftarrow \sum_{j=1}^M \beta^j \mathbf{s}^j$
- 19: **return** \mathbf{v}

AttentiveChrome Details: AttentiveChrome Forward Propagation algorithm is presented in Algorithm box S:1, while Figure S:2 presents the overview of the proposed AttentiveChrome in detail.

References

- [1] Sepp Hochreiter and Jürgen Schmidhuber. Long short-term memory. volume 9, pages 1735–1780. MIT Press, 1997.
- [2] Ritambhara Singh, Jack Lanchantin, Gabriel Robins, and Yanjun Qi. Deepchrome: deep-learning for predicting gene expression from histone modifications. *Bioinformatics*, 32(17):i639–i648, 2016.

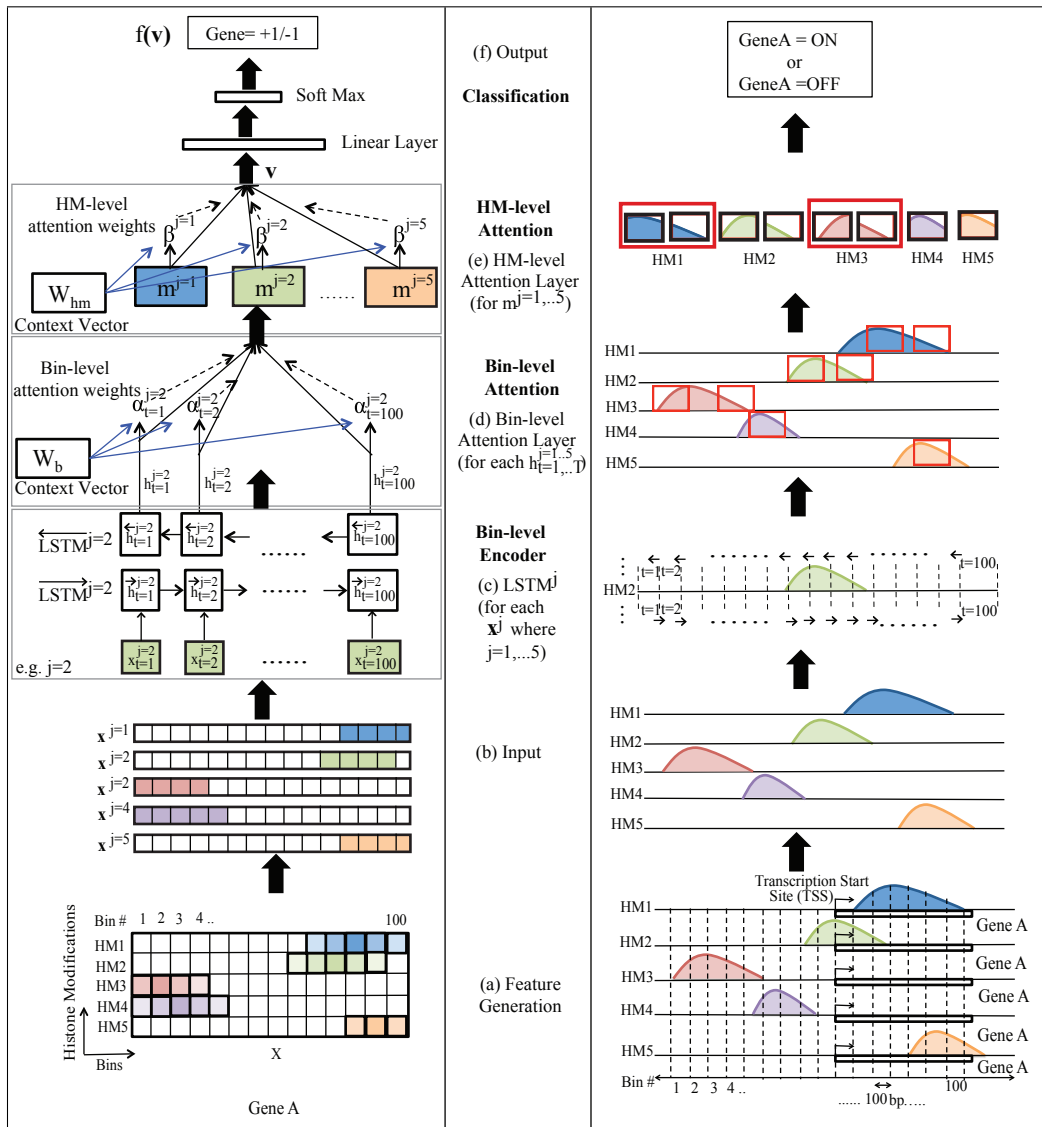


Figure S:2: Overview of the proposed AttentiveChrome, a unified framework that can both predict and understand how histone modifications regulate gene expression. We present six steps in order: (a) We generate an input matrix X for each gene's TSS flanking region, consisting of 100 bins as rows and 5 histone modification (HM) signals as columns. (b) We split the matrix into five vectors representing each HM mark. We input these vectors into the AttentiveChrome model. (c) We use a separate LSTM to learn feature representations of an HM mark. (d) A bin-level attention layer is learned to extract bins that are important for representing an HM mark. This attention layer will aggregate important bins to form an embedding vector for an HM. Here we only show the case of HM2 in steps (c) and (d). (e) Next, to capture the dependencies among different HM marks, we apply another LSTM layer over the representation of 5 HMs. (f) To reward HM marks that are significant clues for classifying an individual gene's expression, AttentiveChrome adds another attention layer- HM-level attention. This layer outputs an embedding vector v for the whole gene region under consideration. (g) Finally, the output embedding v from the previous layers will be fed into a classification module to predict the gene expression as high(+1)/low(-1).